IOP Conference Series: Materials Science and Engineering

PAPER • OPEN ACCESS

Numerical Analysis on Bond Strength of FRP Re-bars under Elevated Temperature

To cite this article: M H Jamalan and Dr F Fu 2018 *IOP Conf. Ser.: Mater. Sci. Eng.* **371** 012013

IOP Conf. Series: Materials Science and Engineering **371** (2018) 012013 doi:10.1088/1757-899X/371/1/012013

Numerical Analysis on Bond Strength of FRP Re-bars under Elevated Temperature

M H Jamalan[1] and Dr F Fu[2]

1 PhD Student, City University of London, London, UK
2 Lecturer in Structural Engineering, City University of London, London, UK
E-mail: abnz631@city.ac.uk

Abstract. The bond behaviour between fibre reinforced polymer (FRP) and concrete at a different temperature, ranging from room temperature (20˚C) to high temperature of up to 300˚C, are modelled using the FEA in this paper. Four different commercially produced FRPs with different bond treatments and the bond properties were study in this temperature range. It is observe that when the temperature increases from 20˚C to 300˚C the FRP's bond strength reduced between 80 and 90%, however, this reduction for steel is only 38% at this temperature range. Also as the temperature increased a reduction in the bond stiffness has occurred.

1. Introduction

In the past few years, the use of Fibre reinforced polymers (FRP) for reinforcing the concrete structures, where steel reinforcement is not suitable because of a highly corrosive environment or where electromagnetic transparency of the structure is required, has been increased. The properties of FRP re-bars are affected in high temperatures, such as where these re-bars face the fire or even in an extremely hot climate. As the temperature increased the mechanical properties of the polymers, especially their strength and stiffness decrease significantly and the polymer approaches its glass transmission temperature T_g [1]. Different type of polymers are used as the matrix materials in FRP re-bars, the most common polymers are thermosetting polymers like; vinyl ester and polyester. The glass transition temperatures for these polymers are in a range of 60-130˚C. Therefore it can be expected that if the temperature approaches or passes the glass transition temperature of the polymer resin the mechanical properties of the FRP re-bars will be affected.

High-performance inorganic and organic fibres, such as glass, carbon, and aramid fibres, are being used in FRP re-bars [2]. These fibres exhibit good mechanical property retention in the elevated temperature range considered in this work (up to 250˚C) [3], and it is expected that failure of the re-bars at high temperature will occur first in the polymer matrix [4], studied the properties of the FRPs at high temperatures, as the result of these test on a variety of the FRP re-bars they found that the tensile strength of glass and carbon FRP re-bars approximately reduced 20% at a temperature of 250˚C. However, this reduction was more significant for aramid FRP re-bars and it was about 60% at 250˚C. Also, the tests showed that the effect of matrix composition is relatively small. Fujisaki et al. (1993) [5] reported a reduction of 40% in the tensile strength of glass-carbon FRP grids at a temperature of 100˚C, probably due to changes in the properties of the polymer that forms the grid; however, no further reduction was seen for higher temperatures of up to 250˚C. The impact resistance of concrete members (curtain walls) reinforced with the FRP grids at high temperature was good, and concluded that these concrete members would perform satisfactorily in the event of a fire. Wolff and Miesseler (1993) [6] proposed giving pre-stressed concrete members reinforced with glass FRP tendons the same consideration for fire protection as that given for steel tendons, due to the small reduction in the tensile strength of glass FRP tendons, which was similar to that seen for steel tendons.

On the other hand, Wang and Evans (1995) [7] reported a reduction of 75% in the flexural strength of FRP beams as the temperature was increased from room temperature to 300˚C. Okamoto et al. (1993) [8] investigated the performance of the pre-stressed concrete beams in a fire. In their test, the pre-stressing tendons were made of aramid FRP, and the reinforcement was made of either aramid or carbon FRP re-bars. As the temperature of the reinforcements reached approximately 200˚C and 300˚C for the aramid and carbon rods, respectively, Failure of the beams has occurred.

The variation in these results can be explained by the differences in the properties of FRP composites in different orientations, these discrepancies in orientation are because of the anisotropy of the composite material. In the direction of the fibres (i.e., the longitudinal or axial direction of the rebar), the properties are governed by the properties of the fibres, which exhibit good performance at high temperature. The polymer largely governs the properties in the transverse direction, such as shear in a plane parallel to the fibre direction. Therefore a reduction in the shear strength of an FRP rebar is expected as the temperature increases. This reduction explains the aforementioned results of Wang and Evans (1995) [7], as the flexural strength of a composite beam relies on the transfer of shear stress through the polymer.

2. Numerical programme

2.1. Rods

In this paper four types of FRP re-bars were modelled and compared with steel re-bars. The used FRP re-bars are shown in Figure 1. Each FRP re-bars have a dimeter of 12.7 mm, and the diameter of the steel bar was 12.0 mm. The actual diameter of the FRP re-bars was slightly larger, depending on the surface treatment of each one. Properties of the FRP re-bars are given in Table 1.

Each FRP re-bars have different surface treatments in order to study the bonding between the FRP re-bars and concrete as can be seen in Figure 1. Surface of the CB re-bar is covered by a moulded polymer giving this bar lugs with similar geometry as those found on steel reinforcing bars. For other FRP re-bars a helical braid of glass fibres was wound to cover the surfaces of the bars. The braid was wider for CPI compared to CPH and NG re-bars as shown in Figure 1. In addition, for producing a large convex protrusions on the surface of the re-bars the braid was wrapped tightly around the NG bar. To increase the bond between the FRP re-bars and the concrete embedded sand particles on the surface of the CPH and NG re-bars was used. The sand was dispersed evenly on the surface of the CPH re-bar in a very thinner layer of polymer compared to NG re-bar.

2.2. Concrete

Normal strength concrete was used in this study. Table 2 shows the general properties of concrete such as, mass density, young’s modulus and Poisson’s ratio. Also, concrete damage plasticity properties has been tabulated in Table 3 (a and b).

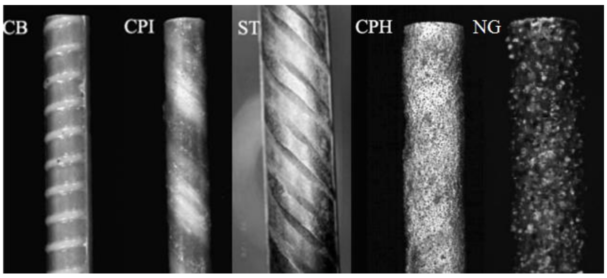

Figure 1. Tested re-bars.

Table 1. Properties of tested FRP re-bars.

Bar Type	Diameter (mm)	Type of Resin	Physical bond improvement to surface of bars	Space between deformations (mm)	Glass transition temperature (˚C)
CB	12.7	Urethane modified vinyl ester	Large deformations	7.5	124
CPH	12.7	Epoxy vinyl ester	Helix + sand coating	27	122
CPI	12.7	Epoxy vinyl ester	Helix + resin roughening	25	95
NG	12.7	Polyester	Helix + sand coating + deformations	12	60
ST	12	Steel	Large deformations	7.7	–

Table 2. General properties of concrete.

Mass Density [kN/mm^3]	**Elasticity**	
	Young's Modulus [N/mm^2]	Poisson's Ratio
2.36×10^{-5}	24855.578	0.2

Table 3 (a). Concrete damage plasticity properties.

Plasticity				
Dilation Angle	Eccentricity	f_{b0}/f_{c0}	K	Viscosity Parameter
36	0.1	1.16	0.666	0

Table 3 (b). Concrete damage plasticity properties.

Compressive Behavior		**Tensile Behavior**	
Yield Stress	Inelastic Strain	Yield Stress	Cracking Strain
5.3	0	0.984219488	0
5.49	0.000222	1.524994267	9.6E-005
22.93	0.001083	1.296676701	0.000144
28.99	0.00174	1.155729537	0.000192
30	0.002219	1.057041912	0.00024
27.11	0.003355	0.982697179	0.000288
22.83	0.004438	0.923934094	0.000336
21.71	0.004719	0.875879203	0.000384
		0.835570706	0.000432
		0.801087969	0.00048
		0.771122074	0.000528

IOP Conf. Series: Materials Science and Engineering **371** (2018) 012013 doi:10.1088/1757-899X/371/1/012013

	0.744745197	0.000576
	0.721278303	0.000624
	0.700211106	0.000672
	0.681151482	0.00072
	0.663792309	0.000768
	0.647889051	0.000816
	0.63324418	0.000864
	0.619696109	0.000912
	0.607111153	0.00096
	0.595377601	0.001008
	0.584401251	0.001056
	0.57410202	0.001104
	0.564411316	0.001152
	0.555269995	0.0012

3. Analysis

The pull-out simulation were performed in accordance to ACI440.3R-04 and CSA S806-02 standards in ABAQUS as shown in Figure 2. This is an implicit analysis procedure suitable for modelling both material and geometric nonlinearities was used, contact between different parts was also modelled. The FE analysis comprised an elastic-plastic simulation of the pull-out process and the determination of the load-displacement curve in the steel/GFRPs bars. Appropriate boundary conditions were applied to the model.

The rods were embedded vertically in a concrete block with a dimension of $200 \times 200\ mm$ and the length of $200mm$. Embedded length (l) was $63mm$ (5 diameters) following a bond breaker zone of $63mm$. The layout of the concrete block has been shown in Figure 3.

The bottom surface of the model will be fully constrained along the concrete portion, but leave the steel/FRPs bars free. Far field displacements are also constrained due to limited influence of the pull-out loading.

The FE simulations were conducted for all the models and the FE results were compared with previous experimental works that have been done by (Baena .M. et al., 2009) [9] on bond behaviour between concrete and FRP bars, (Nanni .A. et al., 2005) [10] on thermal effects on bond between FRP re-bars and concrete and (Tastani .S. P and Pantazopoulou .S. J, 2006) [11] on bond of GFRP bars in concrete.

The FE mesh was uniform and was generated using a solid element which is an 8-node linear, the block after meshing has been shown in Figure 4. The concrete damaged plasticity model was assumed for the normal strength concrete. The concrete damaged plasticity model is based on the assumption of scalar (isotropic) damage, and is designed for applications in which the concrete is subjected to arbitrary loading conditions.

The average bond strength was determined by dividing the maximum pull-out load (P_{max}) by the embedded surface, assuming a uniform bond stress distribution along the rod, this is shown in equation 1.

$$\tau = \frac{P_{max}}{\pi d l} \qquad (1)$$

Where P_{max} is the peak load, d the rod's diameter, and l is the embedded length.

IOP Conf. Series: Materials Science and Engineering **371** (2018) 012013 doi:10.1088/1757-899X/371/1/012013

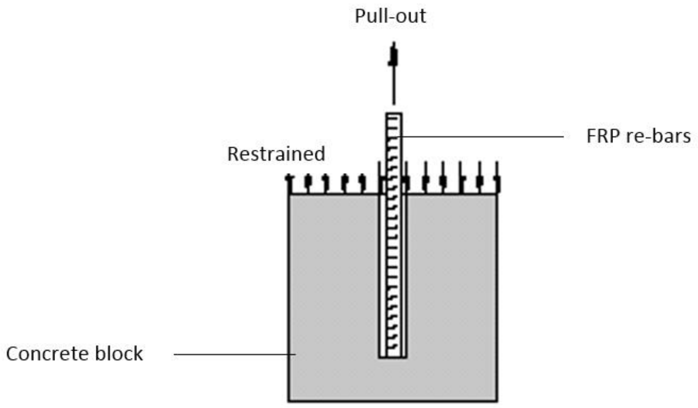

Figure 2. Pull-out test setup.

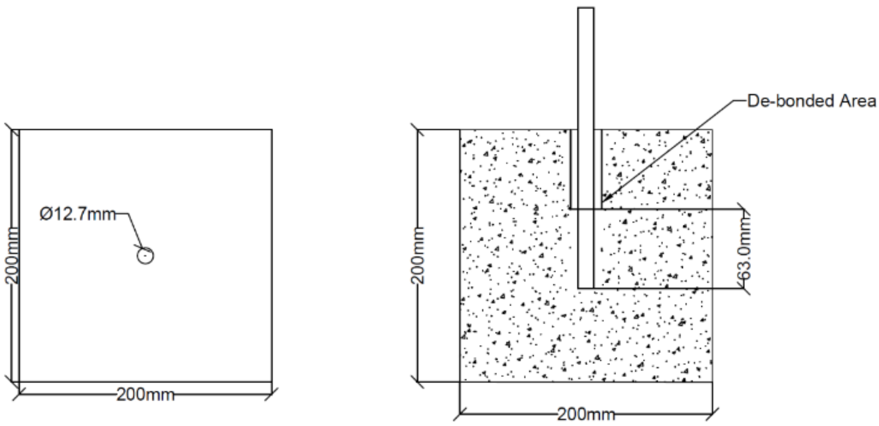

Figure 3. Concrete block layout.

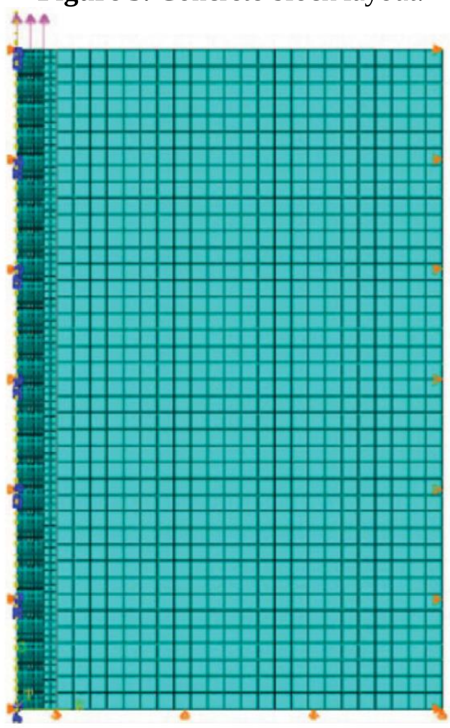

Figure 4. Mesh of the ABAQUS model.

IOP Conf. Series: Materials Science and Engineering **371** (2018) 012013 doi:10.1088/1757-899X/371/1/012013

4. Results

4.1. Bond strength

As it shown in Figure 5, for all bars the effect of temperature on the bond strength calculated by using equation (1)

As it can be seen in Figure 5, all the FRP re-bars behave in a similar manner; except NG re-bar the other FRP re-bars shown a relatively high bond strength at room temperature. The calculated bond strengths for of CB, CPH, and CPI re-bars at room temperature were $13.1, 12.1, and\ 10.8\ MPa$, respectively. This value for steel re-bar was $11.2\ MPa$. A reduction in the bond strength was seen for all of the FRP re-bars at temperatures in the range of $80 - 160^{\circ}C$. At nearly $200^{\circ}C$ the bond strength has not changed and remained almost constant as the temperature was increased. Analysis were stopped at around $300^{\circ}C$. According to (Gentry et al. 1999); at higher temperatures (400˚C and above) the polymer matrix will begin to decompose no mechanical properties can be expected at these temperatures. Table 4 shows the values for the bond strength at room temperature, the residual bond at high temperature, and the degree of bond strength.

Comparing to other FRP re-bars NG bar has the weakest performance as the temperature increased and lost its bond strength quickly at low temperature. At a temperature of $92^{\circ}C$, Loss of 55% of the bond strength was seen, however, the entire loss of bond strength for NG re-bar was only 80% compared with the other FRP re-bars ($85-92\%$). For CB re-bars rapid reduction in bond strength was seen and most of the reduction was seen in a temperature ranging between $80-150^{\circ}C$. This reduction for the CPH and CPI re-bars occurred in a wider range and extended up to $200^{\circ}C$.

As the temperature increased the reduction in bond strength was also occurred in steel. Loss of bond strength was only 40% for the steel re-bar as the temperature reaches $200^{\circ}C$, this value for FRP re-bars was 80% and more. As the temperature increased loss of bond strength for the steel re-bar increased gently. These findings are in good agreement with the findings of Diederichs and Schneidwe (1977) [12].

Effect of the temperature on the strength of the concrete was shown in Figure 6. Reduction in the strength of the concrete can affect the reduction in the bond strength of steel/FRP re-bars. As the temperature reaches $200^{\circ}C$ the concrete strength reduced 15%, with some increase thereafter. These findings are typical of the behaviour of concrete at high temperature as described by Malhotra (1982) [13]. Therefore, some of the reduction in bond strength at high temperature for steel/FRP re-bars can be explained by a reduction in the concrete strength where the bond mechanism is mainly via the concrete.

Covering the surface of the FRP re-bars by inorganic components (i.e., sand particles and helical fibre) add extra resistance to the re-bars when the temperature rises. In CB and NG re-bars, where the bond relies on the properties of the polymer the effect of the elevated temperature was more critical, than for the CPH and CPI re-bars where the helical wrap of glass fibres was used. The performance of the CPH re-bar that had sand particles at the surface was similar to the CPI re-bars where no sand was used at the surface, therefore The effect of the sand particles is not clear.

4.2. Complete pull-out load-slip curve

Figure 7 shows the load vs slip of the tested re-bars at different temperature. Load vs slip curves divided in two part for analysis: pre-peak and post-peak as the temperature rises.

4.3. Pre-Peak behaviour

The slope of the load-slip curve in pre-peak stage can be considered to be the bond stiffness because it gives a relationship between load and deformation. This value has a great impact on the width of primary flexural cracks in reinforced concrete and on the deflection of beams and slabs. As the temperature rises for all the tested re-bars a reduction in the slope of the ascending curve was seen. For all of the FRP re-bars this reduction appears to be linear.

In most design codes and guidebooks, assumed that re-bars are a homogenous materials while describing the bond between the reinforcements and concrete, which means reinforcements are much stiffer than the surrounding concrete. This assumption is appropriate for structures that have been reinforced by steel bars. However, in the case of using FRP re-bars as the reinforcing bars, this assumption is not true, because FRP re-bars are weaker and more flexible than the concrete, especially when the temperature increases.

4.4. Post-peak behaviour

At room temperature the post-peak behaviour can be divided into two stages: (1) for a short distance after the peak Rapid reduction in the load bearing; and (2) more moderate reduction after that. Using different surface treatments affect the rate of reduction in the load in Stage 1 and the final values of the load and slip in Stage 2. Immediately after the peak load, a steep reduction of $30 - 40\%$ is seen for CB re-bars. A steep post-peak reduction can be still seen at the temperature of $130^\circ C$; however, after that a reduction occurs by a constant low slip. At a higher temperature of $200^\circ C$, a small peak is seen with a gradual decrease thereafter. In this type of re-bars (with lugs) the bond mechanism is rely on wedging of the lugs in the surrounding concrete. As the temperature raises, the surface layer with the lugs softens and becomes more flexible and weak, thus preventing the mechanism of wedging from being effective.

At room temperature CPH re-bar slips $5mm$ at its peak load. This is followed by a moderate reduction thereafter. A moderate reduction was seen as the temperature increased instantly after the peak to a complete reduction of the load. A similar behaviour was seen for CPI and NG re-bars; however, the peak load was lower than what was seen for the CPH rods at room temperature. The slope of the post-peak curve becomes more linear as the temperature increases, and the sudden drop right after the peak disappears. The helical wrapping on the rods and sand particles embedded on the surface of these re-bars caused the differences between the post-peak behaviour of them compared to CB re-bar. In these re-bars the bond mechanism is rely only on the additional features (i.e., the helical wrap and the sand particles), which are less sensitive to the temperature. Therefore the post-peak reduction is more moderate and exhibits constant bond strength to complete pull-out.

Steel re-bar does not show a significant change in behaviour in load-slip curve as the temperature increased. Generally, a rapid decrease of about 50% of the load was seen, after the peak load was reached, followed by a gradual decrease to complete pull-out. As the bond mechanism of steel re-bar are rely on mechanical anchoring to the concrete at all temperatures, so no significant change is expected as the temperature increased, however, for a moderate general reduction resulting from the reduction in the concrete strength as discussed previously.

Table 4. Bond strength value at room temperature, residual bond strength, and amount of bond strength loss

Rod Type	**Bond Strength (MPa)**		**Loss of Bond (%)**
	Room Temperature	Residual Bond	
CB	13.1	1.2	91.6
CPH	12.1	1.8	86.2
CPI	10.8	1.7	85.2
NG	4.2	0.9	80.4
Steel	11.1	6.7	38.5

IOP Conf. Series: Materials Science and Engineering **371** (2018) 012013 doi:10.1088/1757-899X/371/1/012013

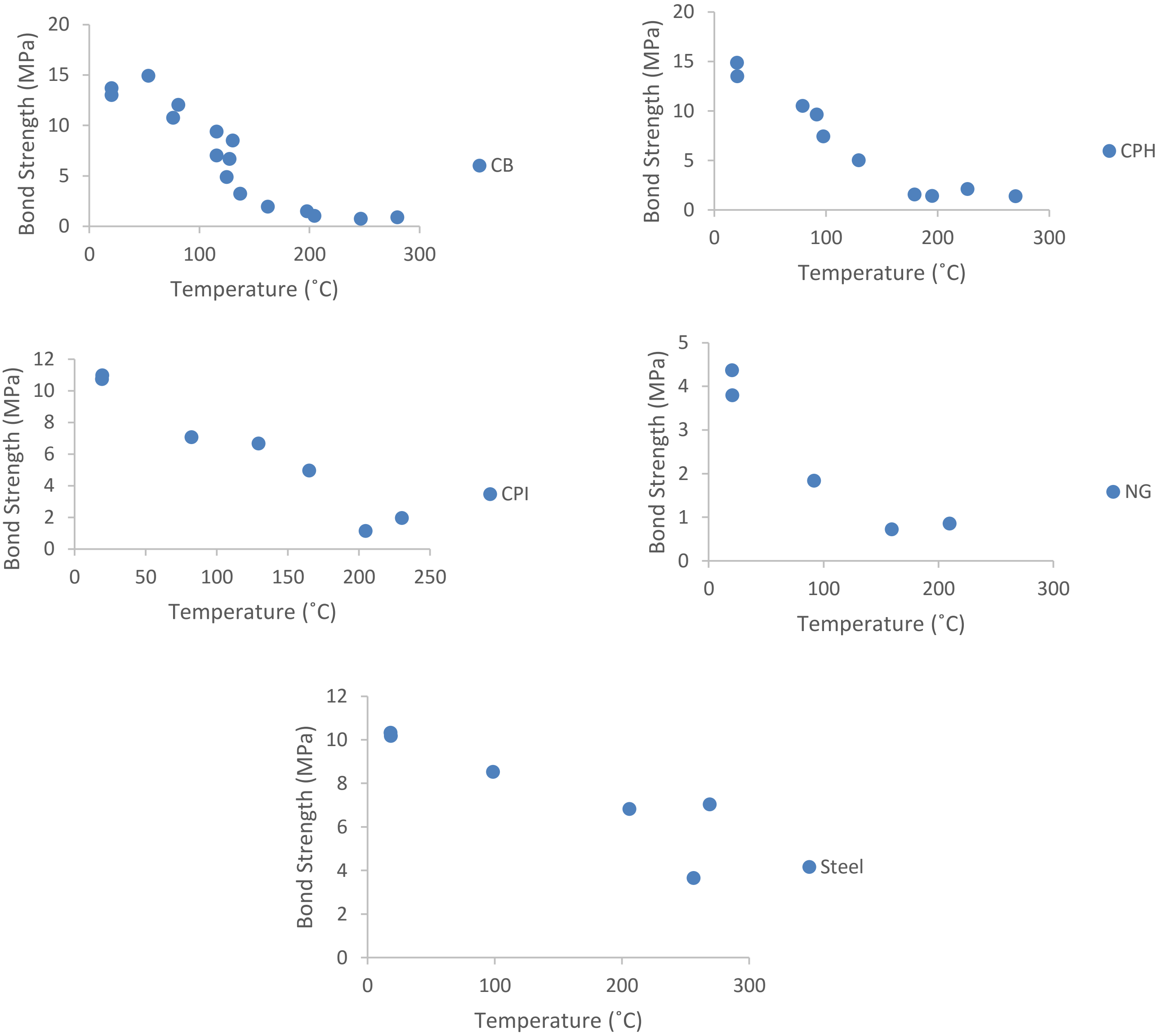

Figure 5. Effect of temperature on tested FRP re-bars.

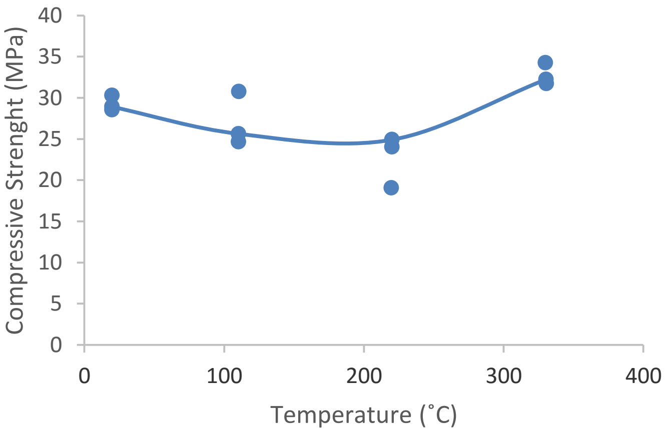

Figure 6. Effect of temperature on concrete compressive strength.

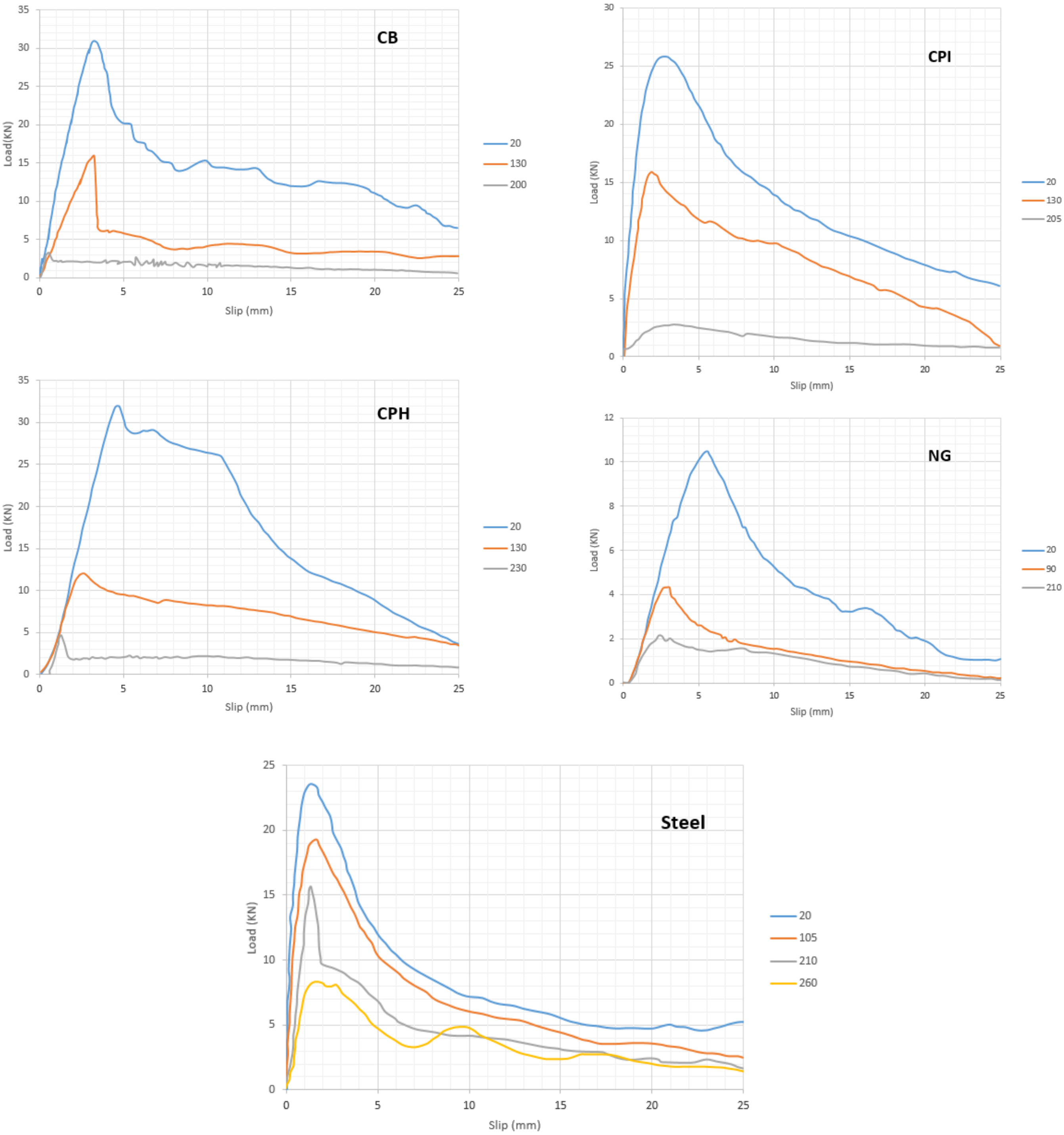

Figure 7. Load-Slip curves for tested FRP re-bars at different temperature.

5. Discussion

It appears that the bond strength of the FRP re-bars are depend on the bond mechanisms of the polymer at the surface of these re-bars at high temperatures. This study showed that in CB and NG re-bars the bond properties are only rely on the polymer. In CB rod a large stiff lugs at the surface provide the bond strength at room temperature, and in NG rod, a thick weak polymeric layer at the surface hides the deformations of the core and does not sufficiently support the sand particles embedded on the surface, which were presumably provided to enhance the bond. As the temperature

increased a rapid reduction in bond strength was seen in both cases. However, in the post-peak behaviour the differences between these two re-bars can be seen.
CPH and CPI re-bars, where wrapped by helical glass fibre with a thin layer of polymer shown a better behaviour in bonding system. As the temperature increased the reduction in bond strength was more moderate, and in the post-peak stage the behaviour was more gradual reduction in the load bearing rather than a sudden drop, compared by the CB re-bar.
At elevated temperature concrete losses some of its strength due to internal vapour pressure, this reduction in strength can affect the reduction in the bond strength between the concrete and reinforcing bars as it was seen in steel.

6. Summery and conclusion

Different types of FRP re-bars were tested for pull-out at temperatures of up to $300^{\circ}C$. In all FRP re-bars high values of bond strength were obtained at room temperature, except for the one which had a weak external layer. The bond strength of all other FRP rods were as high as or higher than the steel rods.
The results showed that as the temperature increased, bond strength reduced massively. In CB rod this reduction was 92% and the bond strength dropped from 13.2 to 1.1 MPa. The polymeric lugs creates a bond between this type of rod and concrete, which appear to be better than other re-bars at high temperature. Having helical wrapping of glass fibre around the core of CPH and CPI re-bars, reduced the reduction in bond strength (from 12.2 to 1.7 MPa and from 10.9 to 1.6 MPa, respectively), however, at high temperature the value of the bond strength was very low for all of the FRP re-bars. In the same temperature range the reduction in the bond strength of the steel re-bar, in comparison, was from 11.2 to 6.9 MPa.
As it seen in NG re-bar a thick polymeric layer at the surface appears to negatively affect the bond both at room temperature and at $200^{\circ}C$.
Temperature also affects the slope of the ascending load-slip curve (the bond modulus), which decreases as the temperature increases. As the temperature increases, the descending curve of the FRP re-bars becomes more linear, indicating a degradation in the polymeric surface treatments that support the bond, leaving the rebar with only a friction mechanism to create a bond.

7. References

[1]. Fried, J. R. (1995). *Polymer science and technology*. Prentice-Hall, Englewood Cliffs, N.J., 167–169.
[2]. Yamaski, Y., Masuda, Y., Tanano, H., and Shimizu, A. (1993). ‘‘Fundamental properties of continuous fiber bars.’’ *Proc., Fiber Reinforced Plastic Reinforcement for Concrete Struct.*, A. Nanni and C. W. Dolan, eds., American Concrete Institute, Detroit, 715–730.
[3]. Dostal, C. A., ed. (1987). *Engineering materials handbook, Vol. 1: Composites*. ASM International, Materials Park, Ohio.
[4]. Kumahara, S., Masuda, Y., and Tanano, Y. (1993). ‘‘Tensile strength of continuous fiber bar under high temperature.’’ *Proc., Fiber-Reinforced- Plastic Reinforcement for Concrete Struct.*, A. Nanni and C. W. Dolan, eds., American Concrete Institute, Detroit, 731–742.
[5]. Fujisaki, T., Nakatsuji, T., and Sugita, M. (1993). ‘‘Research and development of grid shaped FRP reinforcement.’’ *Proc., Fiber-Reinforced- Plastic Reinforcement for Concrete Struct.*, A. Nanni and C. W. Dolan, eds., American Concrete Institute, Detroit, 177–192.
[6]. Wolff, R., and Miesseler, H. J. (1993). ‘‘Glass fiber prestressing system.’’ *Alternative materials for the reinforcement and prestressing of concrete*, J. L. Clarke, ed., Chapman & Hall, London, 34–54, 131 132.
[7]. Wang, N., and Evans, J. T. (1995). ‘‘Collapse of continuous fiber composite beam at elevated temperatures.’’ *Composites*, 26(1), 56–61.
[8]. Okamoto, T., Matsubara, S., Tanigaki, M., and Hasuo, K. (1993). ‘‘Practical application and performance of PPC beams reinforced with braided FRP bars.’’ *Proc., Fiber-Reinforced-Plastic Reinforcement for Concrete Struct.*, A. Nanni and C. W. Dolan, eds., American Concrete Institute, Detroit, 875–894.

IOP Conf. Series: Materials Science and Engineering **371** (2018) 012013 doi:10.1088/1757-899X/371/1/012013

[9]. Baena, M. et al. 2009. Experimental Study of Bond Behaviour Between Concrete and FRP Bars Using a Pull-Out Test. Journal of Composites for Construction,pp. 784-797.
[10]. Nanni, A. et al. 2005. Thermal Effect on Bond Between FRP Rebars and Concrete. Journal of Composites for Construction.pp. 1223-1230.
[11]. Tastani, S.P., Pantazopoulou, S.J. 2006. Bond of GFRP Bars in Concrete: Experimental Study and Analytical Interpretation. Journal of Compusits for Construction. pp. 381-389.
[12]. Diederichs U, Schneidwe U. Untersuchung des Verbundverhaltens und der Verbund-Festigkeit von Rippenstraben und Glatten Rundstaber bei Hohen Temperaturen. Institute Fur Baustoffkundeund
[13]. Malhotra, L. (1982). *Design of fire-resistance structures*. Surrey University Press, London, 48–77.